13. RECORD ANNUAL MEAN WARMTH OVER EUROPE, THE NORTHEAST PACIFIC, AND THE NORTHWEST ATLANTIC DURING 2014: ASSESSMENT OF ANTHROPOGENIC INFLUENCE

Jonghun Kam, Thomas R. Knutson, Fanrong Zeng, and Andrew T. Wittenberg

According to CMIP5 models, the risk of record annual mean warmth in European, northeast Pacific, and northwest Atlantic regions—as occurred in 2014—has been greatly increased by anthropogenic climate change.

Introduction. HadCRUT4v3 observed surface temperature data (Morice et al. 2012) indicate that during 2014, record annual mean warm anomalies occurred in regions of Europe, the eastern North Pacific region (EPac), and the western North Atlantic (WAtl) (Fig. 13.1b). Considering the 5° × 5° grid cells with at least 100 years of coverage, 12% of this area globally set a new warm record during 2014, and *none* set a cold record (Fig. 13.1b). Globally since 1990, there have been almost no cold annual mean records observed at this spatial scale (Knutson et al. 2013). The unprecedented warm surface temperature anomalies in 2014 were accompanied by anomalous atmospheric circulations, changes in seasonal weather, and adverse effects on regional ecosystems (Bond et al. 2015). To explore the possible contributions of anthropogenic radiative forcings to these unprecedented regional warm anomalies, we use a 25-model set of historical all-forcing (anthropogenic + natural) and control (unforced) climate model runs, along with a 10-model set of natural-forcing-only ensemble historical runs from the Coupled Model Inter-comparison Project Phase 5 (CMIP5-All and CMIP5–Nat; Taylor et al. 2012). Many of our methods follow Knutson et al. (2013, 2014), and some descriptive text is derived from these reports with minor modification.

Model-based detection of long-term regional anthropogenic warming. Annual mean temperature anomaly time series extending back to the mid-to-late 1800s for the three regions (Figs. 13.1f–h) are shown in Figs. 13.1c–e. Europe shows a pronounced recent observed warming, particularly since the 1980s, which is well captured by the CMIP5-All ensemble but not the CMIP5-Nat ensemble. The observed trends (black curve in Fig. 13.1g) are generally outside the 5th–95th percentile range of natural-forced trends-to-2012 (blue/purple envelope) that begin before the early 1980s (except for those beginning around 1930 or 1940). The observed trends are generally consistent with CMIP5-All runs (pink/purple envelope) for all trends-to-2012 that start prior to 2000 (Fig. 13.1g).

Observed time series for the EPac and WAtl regions show a mixture of multi-decadal variability and warming trend. The "sliding trend" analyses (Figs. 13.1f and h) indicate that the warming trends over the EPac and WAtl regions are generally indistinguishable from intrinsic variability, except for trends beginning prior to about 1920 for the EPac region and beginning around 1910 for the WAtl region. The observed time series show that the EPac and WAtl regions have relatively strong multidecadal SST variability compared to the long-term trend, and were particularly warm during 1930–60. Including the highly anomalous year 2014 in the observed trends (Figs. 13.1f–h, white dashed) does not change the main conclusions, except that EPac trends beginning around 1950 become marginally detectable, according to the models.

Thus according to CMIP5 models, the long-term warming over Europe is likely attributable in part to anthropogenic forcing, as it is consistent with the CMIP5-All runs but generally inconsistent with CMIP5-Nat, with some dependence on the start year for the trend. Meanwhile, due to strong intrinsic variability, the long-term warming over the EPac and

AFFILIATIONS: Kam—NOAA/Geophysical Fluid Dynamics Laboratory, and Program in Atmospheric and Oceanic Sciences, Princeton University, Princeton, New Jersey; Knutson, Zeng, and Wittenberg—NOAA/Geophysical Fluid Dynamics Laboratory, Princeton, New Jersey

DOI:10.1175/BAMS-D-15-00101.1

A supplement to this article is available online (10.1175/BAMS-D-15-00101.2)

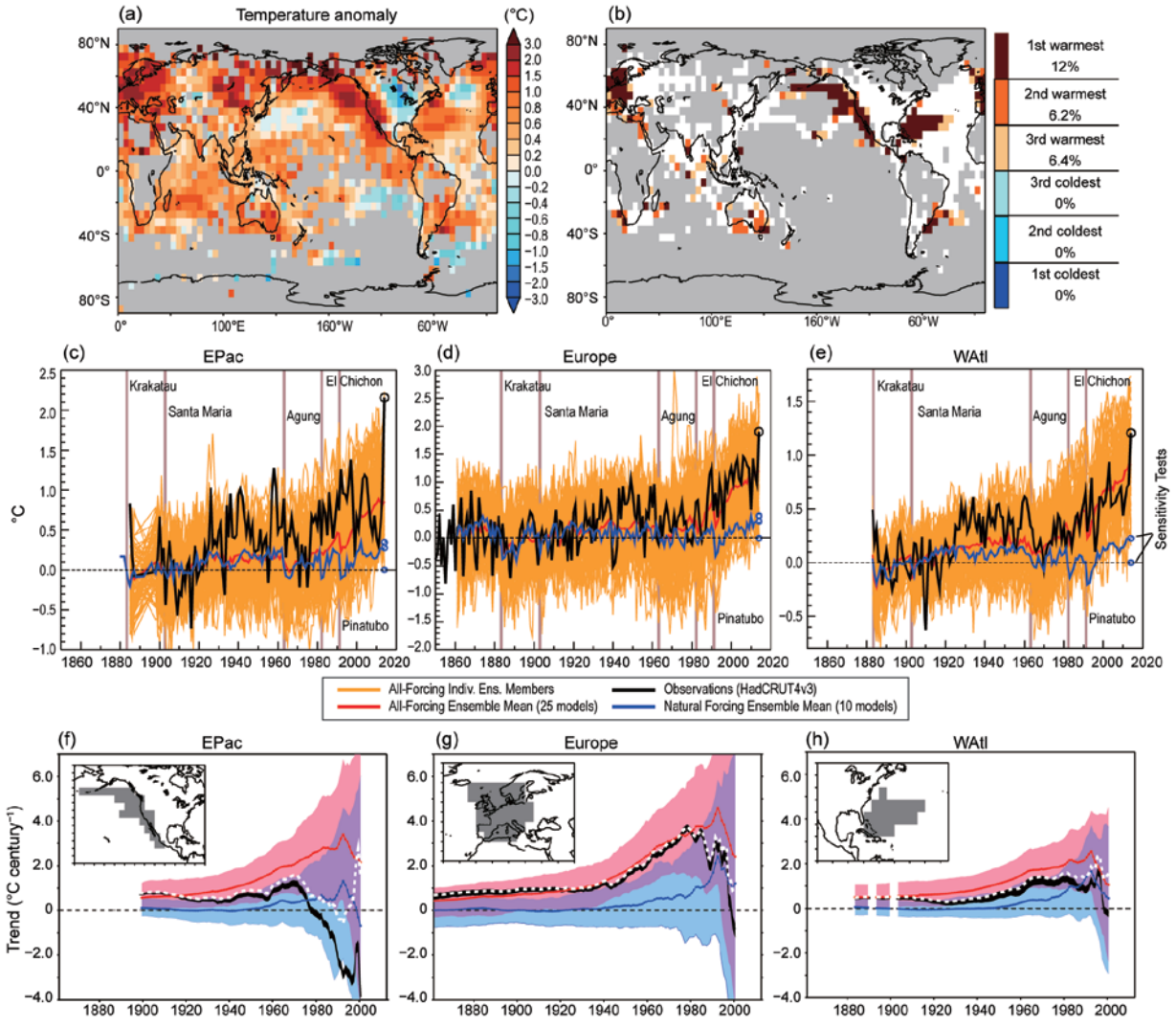

Fig. 13.1. (a) Annual mean surface air temperature anomalies (°C) for 2014 (1961–90 base period) from the HadCRUT4 dataset. (b) Colors identify grid boxes with annual mean anomalies that rank 1st (dark red), 2nd (orange-red), or 3rd (yellow-orange) warmest in the available observed record. Gray areas did not have sufficiently long records, defined here as containing at least 100 available annual means, which require at least four available months. (c)–(e) Annual mean surface temperature anomalies (°C) for the eastern Pacific, Europe, and western Atlantic regions. Black curves: observed (HadCRUT4) anomalies; dark red (dark blue) curves: ensemble anomalies for CMIP5-All (CMIP5-Nat) runs, with each available model weighted equally; orange curves: individual CMIP5-All ensemble members. Blue circles labelled N_{low} (zero), N_{mid} (the modeled temperature anomaly for 2012), and N_{high} (the maximum over the full period) depict three estimates of the CMIP5-Nat response for 2014. CMIP5-All time series are extended as needed with data from RCP4.5 runs. All time series adjusted to have zero mean over the period 1881–1920. (f)–(h) Trends to 2012 [°C (100 yr^{-1})] in the regional series in (c–e) as a function of starting year. Black, red, and blue curves depict observations, the CMIP5-All ensemble mean, and the CMIP5-Nat ensemble mean, respectively. Pink envelope (blue-region) depicts the 5th–95th percentile range of trends from the CMIP5-All (CMIP5-Nat) runs. Purple shading indicates pink- and blue-region overlap. White dashed curves depict observed trends ending in 2014, rather than 2012. Maps indicating the three regions are shown in (f–h).

WAtl regions is generally not clearly attributable to anthropogenic forcing.

Model-based attribution of the 2014 regional annual mean extreme warm anomalies. To assess the contribution of anthropogenic forcing to the 2014 extreme temperature anomalies, we first constructed histograms (Figs. 13.2a–c) of HadCRUT4v3 observed anomalies (black distributions) and "observed residuals" (solid green distributions). The observed

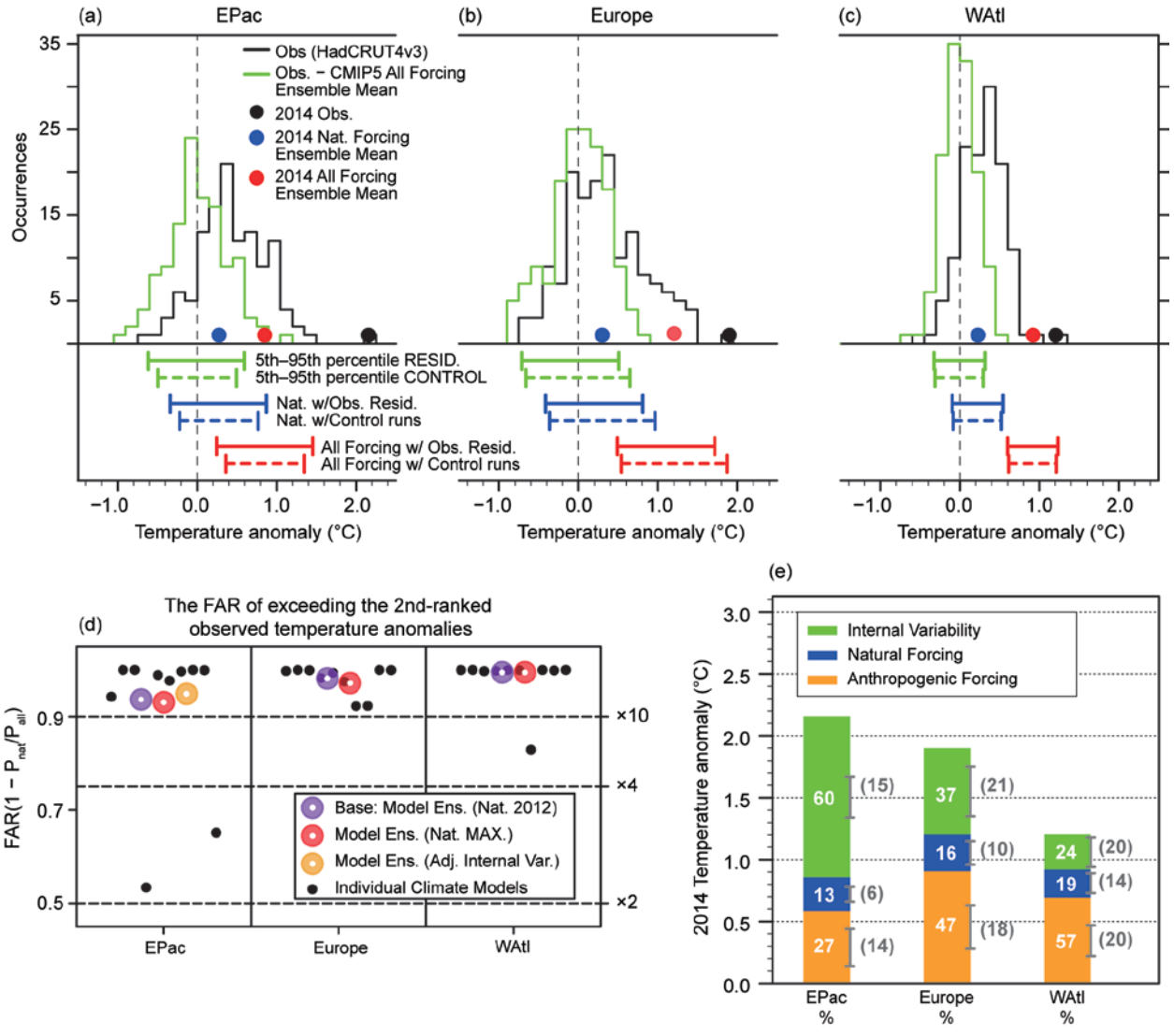

Fig. 13.2. (a)–(c): Histograms of "observed residuals" (solid green lines) and observed annual mean temperature anomalies (black lines) over the three regions. Observed residuals obtained by subtracting CMIP5-All forcing ensemble means from observations and then subtracting any remaining long-term mean. The 5th to 95th percentile ranges of observed residuals and control run variations are depicted by green solid and dashed error bars. Blue (red) error bars depict the 5th–95th percentiles of observed residuals and CMIP5-Control runs, respectively, offset by ensemble means for 2014 from CMIP5-Nat (CMIP5–All) simulations. Black, red, and blue dots in (a)–(c) depict observed, CMIP5-All, and CMIP5-Nat anomalies for 2014. (d) Estimates of the FAR of exceeding the second-ranked observed temperature anomalies from the CMIP5 multimodel ensemble (large purple circle) and its uncertainty (black solid circles) as estimated from the 10 paired CMIP5-All and CMIP5-Nat runs from individual CMIP5 models. Large red circles depict FAR sensitivity tests using—for the 2014 CMIP5-Nat value—the maximum temperature anomalies in any one year from the CMIP5-Nat multimodel ensemble means (online supplemental material); large yellow circle shows a test using adjusted (+22%) internal variability over the EPac region. Dashed lines labeled "×10", "×4", and "×2" indicate risk ratios (probability of occurrence in the CMIP5-All vs. CMIP5-Nat distributions). (e) Stack bars show the estimated contributions of anthropogenic forcing (CMIP5-All – CMIP5-Nat; orange), natural forcing (CMIP5-Nat; blue), and internal variability (Obs. – CMIP5-All; green) to 2014 anomalies (relative to 1881–1920) over the three regions. Standard errors of the various contribution estimates are given in parentheses with ±1 standard error ranges depicted by gray error bars (online supplemental material).

residuals, obtained by subtracting the CMIP5-All multimodel mean from observations, are an estimate of "observed" unforced climate variability which can be compared to the model control runs. Figure 13.2a–c compares the 5th–95th percentiles of the observed residuals (green solid bars) and the CMIP5

Control runs (green dashed bars). Fig. 13.2a–c also shows these ranges shifted by the magnitude of 2014 annual mean forced anomalies as derived from either CMIP5-Nat (blue bars) or CMIP5-All (red bars) ensemble means (see online supplemental material). The observed 2014 anomalies (black solid circles) for all three regions are far beyond the 95th percentile of the observed residuals, or the CMIP5 Control or CMIP5-Nat. distributions; for the EPac and Europe regions they are even beyond those from the CMIP5–All distributions. The 2014 observed anomaly over the WAtl region is near the 95th percentile of the CMIP5-All distribution. These results indicate that the 2014 annual mean anomalies over all three regions are extremely unusual compared to model-simulated natural variability, and over the EPac and Europe regions are even unusual compared to CMIP5-All runs (though the latter runs including anthropogenic forcing are closer to the observations). Modeled internal variability compares fairly well to the observed residual variability, though Fig. 13.2a suggests a ~20% underestimate of internal variability of annual means by the control runs in the EPac region. This possible underestimate does not markedly affect our conclusions about the 2014 extremes, as discussed below.

To assess the contribution of anthropogenic forcing to the risk of extremes like 2014, we estimated the fraction of attributable risk (FAR) for extreme anomalies in each region, using annual mean temperature anomaly distributions derived from the CMIP5-All, CMIP5-Nat, and control runs. The FAR compares the event probability (P) between the CMIP5-Nat and CMIP5-All runs ($FAR = 1 - P_{nat}/P_{all}$). Our FAR estimates address the question of attribution specifically for the three regions with highly anomalous warmth in 2014, and are not intended to be representative of global behavior or of other regions or years in general.

Observed annual mean anomalies for 2014 and an alternative (second-ranked) year are used as alternative extreme-event thresholds in our FAR analysis. The simulated probabilities of exceeding the observed 2014 anomalies over the EPac, Europe, and WAtl regions are 0.2% (0.1%), 4% (0.1%), and 5% (0.2%) based on distributions derived from the CMIP5-All (CMIP-Nat) runs, respectively, and using control-run-estimated internal variability. Therefore, the initial FAR estimates for anthropogenic forcing are 0.42, 0.97, and 0.96 for the EPac, Europe, and WAtl regions, respectively. However, the record 2014 events are far out in the tails of the modeled distributions. The EPac has a particularly long "warm tail" in the modeled internal variability distribution (not shown) which causes some instability in the FAR estimates for high thresholds like 2014. Therefore, we also examined the occurrence rates and FAR of the observed temperature anomalies using the second-ranked anomalies (1997, 2006, and 2003 over the EPac, Europe, and WAtl regions); the probabilities are 4% (0.2%), 26% (0.4%), and 46% (0.2%) for the CMIP5-All (CMIP-Nat.) runs, respectively. Using these thresholds, the FAR estimates are 0.94, 0.98, and 0.99, for the EPac, Europe, and WAtl regions. Sensitivity tests (Fig. 13.2d) were done using alternative estimates of the Natural Forcing 2014 contribution (N_{mid} and N_{high}) from CMIP5-Nat runs (large red circles), or adjusting (increasing) the simulated internal variability over the EPac region by the factor 1.22 (large orange circle); these confirm that our FAR estimates for the second-ranked-year thresholds are robust to these assumptions. Uncertainties in the FAR estimates were also explored by computing the spread of results across individual CMIP5 models (Fig. 13.2d; methods described in online supplemental material). These sensitivity tests show that, using the second-ranked-year threshold values, the estimated FAR is above 0.9 for all 10 individual models for Europe. For the WAtl and EPac, nine and eight of the 10 models have FAR above 0.9, respectively.

We evaluate, using CMIP5 models, the contributions of different factors to the observed annual mean temperature anomalies for 2014 (Fig. 13.2e). The 2014 annual mean anomalies (relative to 1881–1920) for the EPac, Europe, and WAtl regions are 2.2°, 1.9°, and 1.2°C, respectively. For the three regions, the model-derived central estimates of external forcing (anthropogenic + natural) contributions to these observed anomalies are: 0.85°, 1.2°, and 0.9°C; for natural forcing only: 0.28°, 0.3°, and 0.22°C; and for internal variability: 1.35°, 0.7°, and 0.3°C. Thus the portion of extreme 2014 annual mean anomalies attributable to internal variability is about 60%, 37%, and 24% for the EPac, Europe, and WAtl regions, respectively. Also, according to the CMIP5 multimodel ensemble, about 40%, 63%, and 76% of the 2014 annual mean anomalies over the EPac, Europe, and WAtl regions are attributable to natural and anthropogenic forcing combined. Finally, About 27%, 47%, and 57% (13%, 16%, 19%) of the anomaly magnitudes are attributable to anthropogenic forcing (natural forcing) alone. The standard errors of these estimates due to intermodel differences (Fig. 13.2e, gray/parenthesis; see online supplemental material) suggest that the

anthropogenic contribution estimates are relatively robust across the models.

Conclusions. According to the CMIP5 models, the *risk* of events surpassing the extreme (second-ranked) thresholds set in 1997, 2006, and 2003 over the EPac, Europe, and WAtl regions is almost entirely attributable to anthropogenic forcing, with FAR above 0.9 for the ensemble model and almost all of the 10 individual models examined. The strongest model-based evidence for detectable long-term anthropogenic warming was found for the European region, while the case is not as compelling for the WAtl and EPac regions. In the EPac region, there is some indication that internal variability may be at least modestly underestimated by the model control runs. Nonetheless, interannual variability in this region is estimated to have made a larger percentage contribution to the 2014 anomalies than anthropogenic forcing. Thus, the overall evidence for an anthropogenic contribution to the anomalous 2014 temperatures and long-term trend is stronger for Europe than the other two regions. Uncertainties in the models' estimated forced response and the influence of intrinsic variability remain, due to limitations of climate models, uncertainties in the forcings, and (probably to a much lesser extent) uncertainties in the observed temperatures.

ACKNOWLEDGMENTS. We thank the WCRP's Working Group on Coupled Modeling, participating CMIP5 modeling groups, PCMDI, the Met. Office Hadley Centre, and the Climatic Research Unit, University of East Anglia for making available the CMIP5 and HadCRUT4 datasets. We also thank two anonymous reviewers for helpful comments on the manuscript.

REFERENCES

Bond, N. A., M. F. Cronin, H. Freeland, and N. Mantua, 2015: Causes and impacts of the 2014 warm anomaly in the NE Pacific. *Geophys. Res. Lett.*, **42**, 3414–3420, doi:10.1002/2015GL063306.

Knutson, T. R., F. Zeng, and A. T. Wittenberg, 2013: Multimodel assessment of regional surface temperature trends: CMIP3 and CMIP5 twentieth-century simulations. *J. Climate*, **26**, 8709–8743, doi:10.1175/JCLI-D-12-00567.1.

——, ——, and ——, 2014: Multimodel assessment of extreme annual-mean warm anomalies during 2013 over regions of Australia and the western tropical Pacific. [in "Explaining Extreme Events of 2013 from a Climate Perspective"]. *Bull. Amer. Meteor. Soc.*, **95** (9), S26–S30.

Morice, C. P., J. J. Kennedy, N. A. Rayner, and P. D. Jones, 2012: Quantifying uncertainties in global and regional temperature change using an ensemble of observational estimates: The HadCRUT4 data set. *J. Geophys. Res.*, **117**, D08101, doi:10.1029/2011JD017187.

Taylor, K. E., R. J. Stouffer, and G. A. Meehl, 2012: An overview of CMIP5 and the experimental design. *Bull. Amer. Meteor. Soc.*, **93**, 485–498, doi:10.1175/BAMS-D-00094.1.